This paper appears in IEEE Robotics and Automation Letters (RA-L), 2016.
DOI: 10.1109/LRA.2016.2528293

Sliding-based Switching Control for Image-guided Needle Steering in Soft Tissue

Bita Fallahi[1], Carlos Rossa[1], Ron S. Sloboda[2], Nawaid Usmani[2], Mahdi Tavakoli[1]

***Abstract*—This paper represents a sliding based controller for steering beveled-tip needles to stationary locations in soft tissue in a 2D environment by performing appropriate switches of bevel orientation by 180° axial rotations while the needle is being inserted. Assuming the rotation velocity to be large enough with respect to insertion velocity, the out of plane motions of the needle can be neglected. The proposed controller has a non-model-based structure, which is fed by the needle tip deflection error and its derivative obtained from ultrasound images and outputs the switching pattern as the control law. To analyze the stability and convergence of the error, the kinematic unicycle model for beveled-tip needle motion in soft tissue is employed and the constraints on switching parameters are derived. The performance of the controller in the sense of targeting error and number of switches is verified using an experimental setup to insert the needle into gelatin phantom tissue and ex-vivo biological tissue.**

***Index Terms*—Surgical Robotics: Steerable Catheters/Needles; Nonholonomic Mechanisms and Systems**

I. Introduction

A. Related works

STEERABLE needles have been widely used in minimally invasive procedures such as brachytherapy, biopsy and neurosurgery. In such methods, flexible beveled-tip needles are inserted into human tissue for diagnosis, treatment, or sample removal. In these procedures, accurate control of the needle tip position has a great impact on efficiency. To compensate for errors caused by needle deflection and tissue deformation, intelligent assistant robots can be employed to improve the needle targeting accuracy based on physical models and real-time measurements of the system.

Considering the motion of the needle, the nonholonomic constraints on the needle dynamics limit the steerability of the needle and are highly restrictive. To deal with such constraints, there have been many path planning methods proposed in the literature. From a feedback control perspective, using the needle axial rotation as the control input for controlling the needle motion, the system suffers from under actuation as the needle bends both in y and x directions (equivalently, it has both in-plane and out-of-plane motions) – it is difficult to control two outputs through 1 input. Therefore, controlling the 3D position of the needle tip is a very challenging problem. Viewing the needle insertion system as a control system, the control objective can either be regulation or tracking. In regulation, the goal is to control the needle to travel on as straight path by minimizing needle bending, or to travel on an appropriate curved path to reach a desired and feasible deflection at a given final depth. In tracking, the goal is to control the needle to travel on a curved path that specifies a desired deflection at every depth assuming the path satisfies the nonholonomic constraints.

[1] has proposed a planning algorithm in 2D space with obstacles. Some methods have considered tissue motion and used Markov decision process to find the optimal path [2] [3]. [4] has considered the planning problem in 3D space for a stiff tissue with no obstacles and [5] [6] represent motion planners for 3D environment with obstacles. [7] combines a 2D planner with a sequence of image guided needle rotation which compensates the out of plane motions of the needle. In [8] it is shown that by duty-cycle spinning of the needle, paths with different curvatures can be achieved. [9] represents two methods for duty cycle spinning to overcome hardware limitations such as cable wind-up. In order to have paths with variable curvature, this method is combined with 3D planners in [10] for environments with obstacles. Steering the needle using path planning methods require fast online re-planning, which may be computationally expensive. Moreover, most of the control strategies proposed in literature require some physical models or system parameters for which the effects of model uncertainties should be taken into account.

Other methods utilize different measurement methods such as fiber bragg grating sensors [11], acoustic radiation force impulse imaging method (ARFI) [12] and electro-magnetic tracking [13][14]. In [15], to keep the needle moving as straight as possible the needle is rotated when the needle deflection reaches some predefined threshold. In this method the deflection and the rotation locations are calculated based on the force data and needle's model (flexible beam model) which may encounter uncertainties. Duty-cycle spinning method re-

Manuscript received: August, 31, 2015; Revised December, 19, 2015; Accepted January, 24, 2016.

This paper was recommended for publication by Editor Ken Masamune upon evaluation of the Associate Editor and Reviewers' comments. *This work was supported by the Natural Sciences and Engineering Research Council (NSERC) of Canada under grant CHRP 446520, the Canadian Institutes of Health Research (CIHR) under grant CPG 127768 and the Alberta Innovates - Health Solutions (AIHS) under grant CRIO 201201232.

[1]B. Fallahi, C. Rossa, PhD, and M. Tavakoli, PhD, are with the Department of Electrical and Computer Engineering, University of Alberta, Edmonton, AB, T6G 1H9, Canada. {fallahi, rossa, mahdi.tavakoli}@ualberta.ca

[2]R. S. Sloboda, PhD, FCCPM, and N. Usmani, MD, are with the Cross Cancer Institute and the Department of Oncology, University of Alberta, Edmonton, AB, T6G 1Z2, Canada. {ron.sloboda, nawaid.usmani}@albertahealthservices.ca

Digital Object Identifier (DOI): see top of this page.

quires the maximum needle path curvature which may vary during the insertions due to tissue in-homogeneity. The steering method presented in [10] uses the needle path curvature as a constant model parameter to preform any necessary rotations to move the needle toward the target point. To compensate the effect of tissue in-homogeneity on needle path curvature in [16] online curvature estimation is integrated to 3D planners and duty-cycle spinning. [12] incorporates the on-line and off-line curvature estimation method using ARFI imaging technique for finding the value of variable curvature. The steering algorithm is an optimization based method that uses the updated value of curvature to improve the targeting error.

B. Contributions

The specific application of needle insertion considered in this paper is prostate brachytherapy in which the radioactive seeds are implanted in planned locations in or around the tumor. In such a procedure, not only the tip position but also the needle track during insertion into tissue is important. As the seeds will be implanted during the process of retracting the needle and will therefore be positioned the needle track, it is desired to move the needle on a straight line (seed dosimetry planning software assume unbent needles).

The main purpose of the paper is to study the feasibility of a simple non-model-based technique for a regulating problem to steer beveled-tip needles into a target point in soft tissue. The target point is a 2D point which is specified by a desired defection at a desired insertion depth. To steer the needle to the target point, the proposed algorithm only uses the information from visual feedback and no information about the needle or tissue parameters are involved in the controller structure. Especially, the exact value of the needle path curvature is used extensively in many other papers as a parameter in their planning or control algorithms. However, this parameter can be variable due to the tissue inhomogeneity. In this work, we only require a rough estimate of the curvature. It should be noted that since the value of the curvature is not directly used in the steering algorithm, the algorithm is not sensitive to curvature uncertainties. The parameter tuning process is actually an advantage as it provides a way to trade off deflection errors with the number of rotations. A larger needle tip angle (θ^*) allows for a larger deflection error but reduced the number of switches. Moreover, the proposed steering algorithm is based on needle tip deflection feedback measured from ultrasound images which does not require any special measurements or imaging modalities as the widely available low cost three dimensional ultrasound imaging can be used. Using the proposed method, the maximum targeting error obtained in biological tissue, 1.76 mm, is comparable to position error obtained in the literature as 1.56 mm [12] and 1.11 mm [14].

This paper is organized as follow. Section II presents a review of the unicycle model and introduces the controller structure. In section III the stability of the system and convergence of the error is discussed and the parameter constraints are derived. In section IV the proposed method is experimentally validated and the results are presented. Section V gives a comparison of the proposed method and other methods in the literature.

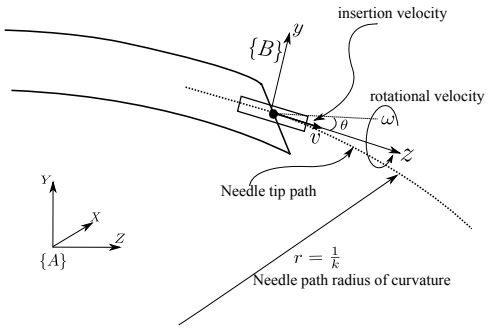

Fig. 1. unicycle model of a beveled-tip needle

II. Proposed controller

A. Unicycle Equations

The kinematics of a bevel tip needle inserted into soft tissue can be expressed using the kinematics of a unicycle moving on a circular path in plane [17] as shown in Fig. 1 :

$$\dot{z} = v\cos\theta \tag{1}$$

$$\dot{y} = v\sin\theta \tag{2}$$

$$\dot{\theta} = kv \tag{3}$$

Here $\dot{(.)}$ denotes the time derivative and z and y represent the position of the needle tip in the $(y-z)$ plane (the insertion direction is z and the orthogonal direction is y, respectively). $\theta \in [-\pi/2, \pi/2]$ gives the needle tip angle found as the anglebetween the z-axis of the moving frame $\{B\}$ attached to the needle tip and the z-axis of the fixed frame $\{A\}$. v is the constant insertion velocity and k denotes the needle path curvature. For a planar motion, k can be written as $\pm k_0$ with $k_0 > 0$ where $\pm$ determines the orientation of the bevel tip, which specifies the concavity of the needle path curve. The bevel orientation can be changed by rotating the needle by $180°$. Using equations (1)-(3), the needle is derived with two inputs, the insertion velocity v and the needle axial rotations, which can be used to steer the needle to the target point. In order to reach the desired deflection, one can perform sequences of $180°$ axial rotations. Assuming the axial rotation velocity to be much larger than the insertion velocity, the out of plane motion can be neglected.

B. Controller Structure

The needles considered in this paper are flexible beveled-tip needles clinically used in prostate brachytherapy. The asymmetric force at the needle tip due to the bevel will cause the needle to bend as it is inserted into the tissue. For clinical reasons (radioactive seed implantation on a straight line), it is desired to steer the needle tip into a target point. In this paper, the target point in the plane is determined either by

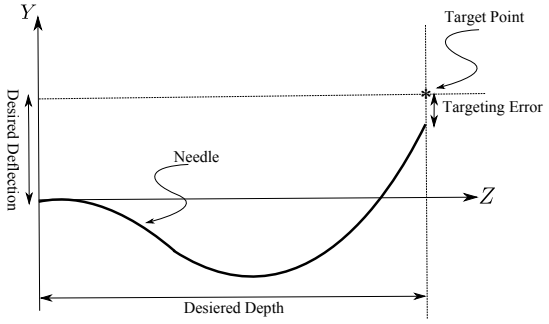

Fig. 2. Target point and the deflection error

a straight line or by a desired deflection at a desired depth. In both cases, the needle targeting error equals the needle tip deflection when the needle reaches the specified depth.

As said above, the error is defined as the difference between the desired deflection and the actual deflection of the needle tip as measured from US images. Fig. 2 shows a schematics of the desired deflection and the deflection error.

In the planar case, since there are only two options available for the bevel orientation, the sequence of axial rotations is determined by switching decisions between the two modes of the system, i.e. mode 1 with $k > 0$ and mode 2 with $k < 0$. Here, we will use sliding mode control to find the switching instants that steer the needle toward the desired position. Let the sliding surface be

$$s = b\dot{e_y} + ce_y \tag{4}$$

in which $e_y = y - y_d$ is the deflection error, y is the needle tip deflection and y_d is the desired deflection. For a constant desired deflection y_d, $\dot{y_d}$ and $\ddot{y_d}$ equal zero and the sliding surface simplifies to

$$s = b\dot{y} + ce_y \tag{5}$$

Starting from zero initial condition, i.e. $y = 0$, $y_d = 0$ is equivalent to moving the needle on a straight path. In the next section, we will show that by proper switching between the two system modes, the stability of the closed-loop system and convergence of the error can be guaranteed.

III. Stability

A. Lyapunov Stability

To analyze the stability of the close-loop system, consider the following Lyapunov function

$$V = \frac{1}{2}s^2 \tag{6}$$

For this positive valued function V, if $\dot{V} < 0$, V and hence $|s|$ will be decreasing. Assuming that $|s|$ is initially bounded and it is decreasing, then s will remain bounded. If the switching is performed such that

$$\dot{V} = s\dot{s} < -\eta|s| \tag{7}$$

for some $\eta > 0$, then s approaches zero [18]. This condition can be written as

$$\begin{cases} \dot{s} > \eta, & \text{if } s < 0. \\ \dot{s} < -\eta, & \text{if } s > 0. \end{cases} \tag{8}$$

Taking the time derivative of (5), we have

$$\dot{s} = b\ddot{y} + c\dot{y} \tag{9}$$

The parameters b and c of the sliding surface need to be chosen to meet (7).

Using (2) and (3), (9) can be written as

$$\dot{s} = v\{\pm bk_0 v\cos\theta + c\sin\theta\} \tag{10}$$

since $\theta \in [-\pi/2, \pi/2]$, the first term in (10) is strictly positive and strictly negative for modes 1 and 2, respectively. Assuming the angle θ is limited to $|\theta| \leq \theta^*$ for some $0 < \theta^* < \pi/4$, choosing the parameters b and c such that

$$\frac{bk_0 v}{c} > \tan\theta^* \tag{11}$$

ensures that $\dot{s} > \eta$ for mode 1 and $\dot{s} < -\eta$ for mode 2 which is appropriate when $s > 0$ and $s < 0$, respectively. In other words, if (11) is satisfied and the switching is performed such that when $s > 0$ the system resides in mode 2 ($k < 0$) at which $s < -\eta$, and when $s < 0$ the system resides in mode 1 ($k > 0$) at which $s > \eta$, (8) will be satisfied. So, choosing the sign of the switching surface as the switching rule makes s and consequently the deflection error to tend to zero.

It should be noted that how fast the tip deflection error approaches zero, i.e. the error dynamics, are determined by parameters b and c. According to (11), since v and k_0 are constant, $\frac{b}{c}$ is lower bounded, which means that the time constant can not be chosen arbitrary. This value should be selected as small as possible as it determines the time constant of error dynamics. For a constant b, a larger value of $\frac{b}{c}$ is equivalent to having a smaller value for c, which reduces the weight of the deflection error in the sliding surface, increasing the required time for the error to approach zero.

In practical applications where the needle is manually inserted into the human body, the surgeon usually performs 1-2 rotations to steer the needle into desired position. This is because surgeons are concerned that too many rotations cause drilling and damaging the tissue and increase trauma to tissue as a result of all the cutting and the heat produced by the needle/tissue friction. This has been previously investigated in the literature [19][20].Since our proposed method is based on sliding mode control, it is desired to keep the sliding surface close to zero. This means that rotations are needed whenever the switching surface changes sign. However, this may cause a chattering in the response, which is equivalent to continuous switching (too many needle rotations). To prevent such a phenomenon, the rotation locations are determined based on a hysteresis framework so that the needle will rotate when the switching surface reaches some switching threshold (and not as soon as it changes sign) as shown in Table I. In this case, a smaller switching threshold is more desirable for containing the needle deflection errors however it increases the number of rotations. For a large switching threshold, the number of rotations are reduced at the expense of increased needle tip deflection errors.

TABLE I
SELECTION OF THE OPERATING MODE BASED ON s

Region	System Mode	$sign(\dot{s})$
$s < -s_s$	Mode 1($k > 0$)	+
$-s_s \leq s \leq s_s$	No mode change	+ or -
$s > s_s$	Mode 2 ($k < 0$)	-

B. Constraints on switching threshold

To find a proper value of s_s, for which the value of θ remains in the desired range $[-\theta^*, \theta^*]$, let $[t_0, T]$ be the time interval between two consequent switches. Since during this interval the system resides in one mode, according to (3) and the switching rule, s and θ will both be monotonic. Therefore, using (5), the variations in s can be written as

$$\Delta s = b(\dot{y}(T) - \dot{y}(t_0)) + c(y(T) - y(t_0)) \tag{12}$$

In this equation, $y(T)$ can be found by integrating (2) and (3), which leads to

$$\theta(T) = kv(T - t_0) + \theta(t_0) = \Delta\theta + \theta(t_0) \tag{13}$$

$$y(T) = \frac{-1}{k}(\cos\theta(T) - \cos\theta(t_0)) + y(t_0) \tag{14}$$

substituting (13) and (14) in (12), the variations in s can be expressed as a function of $\Delta\theta$

$$\Delta s = m_1(\cos\Delta\theta - 1) + m_2 \sin\Delta\theta \tag{15}$$

with

$$m_1 = -\frac{c}{k}\cos\theta(t_0) + bv\sin\theta(t_0) \tag{16}$$

$$m_2 = bv\cos\theta(t_0) + \frac{c}{k}\sin\theta(t_0) \tag{17}$$

Note that m_1 and m_2 are functions of the initial angle $\theta(t_0)$ at the beginning of the switching interval. Taking partial derivative of (12) with respect to $\Delta\theta$, the extremum of Δs occurs at $\Delta\theta_m = \tan^{-1}(\frac{m_2}{m_1})$. From (11), for any $|\theta(t_0)| < \theta^*$, m_2 is positive and the sign of $\Delta\theta_m$ is determined by the sign of m_1. Using the second derivative test for Δs, it can be shown that for $m_1 > 0$, $\Delta\theta_m$ is positive and makes the function Δs to take its maximum, and for $m_1 < 0$, $\Delta\theta_m$ is negative and makes the function to takes its minimum. If the system is in mode 1 ($k > 0$), where $\Delta\theta > 0$, for $m_1 < 0$, the minimum point $\Delta\theta_m < 0$ ensures that Δs will be monotonically increasing with respect to $\Delta\theta$ and its maximum happens at the upper boundary of $\Delta\theta$. In order to have $\Delta\theta_m < 0$ for $k > 0$, the initial condition at the beginning of the switching interval should satisfy

$$\frac{-k_0 bv}{c} < tan\theta(t_0) < \frac{c}{k_0 bv} \tag{18}$$

in which the right hand side is imposed by $m_1 < 0$ and the left hand side is obtained from (11). The same analysis can be done for mode 2 ($k < 0$) which leads to

$$-\frac{c}{k_0 bv} < \tan\theta(t_0) < \frac{k_0 bv}{c} \tag{19}$$

However, since $\theta(t_0)$ at the beginning of each interval is the final result from previous interval, if

$$\frac{bk_0 v}{c} < 1 \tag{20}$$

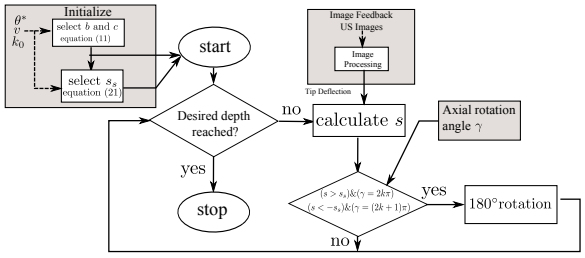

Fig. 3. The procedure of finding the controller parameters and the steering algorithm

both (18) and (19) are satisfied for any $|\theta(t_0)| < \theta^*$ and Δs will be monotonic with respect to $\Delta\theta$ for both $k > 0$ and $k < 0$ which means that $\max|\Delta s|$ happens at $\max|\Delta\theta|$.

Now in order to find the conditions under which θ does not exceed the desired limit θ^*, consider the initial condition $\theta_0 = 0$ and y_0 with $\dot{y}_0 = \ddot{y}_0 = 0$ which leads to $s(0) = ce(0) = c(y(0) - yd)$. At $t = 0$, according to sign$(s(0))$, the system will be in one of the two system modes causing the value of the sliding surface to change until it reaches one of the switching thresholds s_s or $-s_s$. During this phase θ changes from the initial value zero but it is assumed to remain within the desired range. To have such a condition, using (15), s should be selected such that

$$s_s \leq m_1(\cos\theta^* - 1) + m_2\sin\theta^* + s(0) \tag{21}$$

in which m_1 and m_2 are calculated from (16) and (17) for $\theta(t_0) = \theta_0 = 0$. From this relation it can be seen that the initial condition $|s(0)|$ should be small enough to have $s_s > 0$. This inequality gives the upper bound on switching threshold value which ensures that the needle tip angle will not proceed the predetermined angle θ^* to guarantee the stability of the system. The value of θ^* can be determined based on the maximum deflection that the needle is allowed to have. Although choosing larger values for θ^* is equivalent to letting the needle to bend more, it affects the ratio $\frac{b}{c}$ and the maximum allowable value of s_s.

In (21), the initial value $s(0) = ce(0)$ can be used to determine the initial insertion point. For zero initial condition $y_0 = 0$ and zero desired deflection $y_d = 0$ the needle is supposed to move on a straight path. For a nonzero $s(0)$, the needle initial position differs from the desired deflection and the needle is controlled to bends towards the desired deflection.

In summary, selecting a maximum needle tip angle (θ^*) and knowing a rough estimate for the curvature (k_0), the other three parameters (b, cands_s) can be found using (11) and (21). Since these equations involve inequalities, the value of the curvature can be chosen conservatively such that the inequalities result in worst-case values for algorithm parameters. An estimate of curvature can be obtained from previous insertion data and by adding some safety margin, especially when pre-insertions are undesirable. The proposed algorithm and the procedure for finding the corresponding parameters are shown in Fig. 3

IV. EXPERIMENTS

In this section, the steering method introduced in this paper is implemented for needle insertion into phantom and

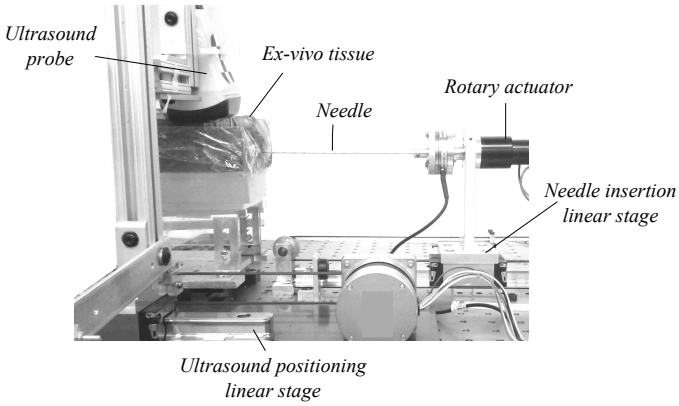

Fig. 4. Experimental setup used to perform needle insertion experiments. The setup provides translational and rotational motions of needle. An ultrasound machine (SonixTouch, Ultrasonix, BC, Canada) is used to track the needle tip position.

biological tissue. The experimental setup used for conducting the experiments is a 2-DOF prismatic-revolute robotic system as shown in Fig. 4. The translational motion of the needle is performed using a carriage actuated by a DC motor through a belt and pulley mechanism. The needle base is attached to a second DC motor, which is assembled on the translational carriage and performs the needle axial rotations. Using the feedback from motor encoders, the position of the motor shaft is controlled using a PID controller. In these experiments, the needle is inserted at a constant velocity [21]. Using the feedback from motor encoders, the position of the motor shaft is controlled using a PID controller. In these experiments the switches between two system modes are performed by 180° axial rotations. The needle used to perform insertions is a standard 18-gauge brachytherapy needle (Eckert & Ziegler BEBIG Inc., Oxford, CT, USA) made of stainless steel, with an outer diameter of 1.27 mm, an inner diameter of 1 mm, and a bevel angle of approximately 20°. The phantom tissue used in the experiments is gelatin made by mixing porcine gelatin powder (Sigma-Aldrich Co., ON, Canada) with water at a temperature of $70^\circ C$. Two different weight ratio of gelatin-to-water mixtures of 15% and 20% are considered for these experiments. As the needle is inserted into tissue, the needle tip is tracked using ultrasound images (SonixTouch, Ultrasonix, BC, Canada). Using the random sample consensus (RANSAC) technique, the needle tip position is estimated from partial observation of the needle in 2D transverse images [22], which is updated every 0.05 sec and is fed back to the controller. The ultrasound probe is attached to a translating platform, which is controlled to track the needle tip position. Here the tissue is considered to have a flat surface, however for non-flat tissue phantoms the translational aspects of the system should be taken into account [23]. To evaluate the performance of the proposed method, five sets of experiments on phantom tissue, with six trials each, and one set of experiment on biological tissue for ten trials are presented. In these experiments, the needle is inserted with a constant velocity and is stopped when the desired depth of 120 mm is reached. To study the effect of the insertion velocity, two different velocities of $v = 2$ mm/sec and $v = 4$ mm/sec are considered for the experiments which are smaller enough than the axial rotation velocity of 5π rad/sec so it is assumed that the needle remains in plane. In each set of experiments only one parameter is changed so the results can be compared for the specific parameter change. In all experiments, the needle is initially inserted for 5 mm to be detectable by ultrasound probe and the initial bevel orientation is assigned to be the same so that the needle initially deflects in the same direction. According to (5), the algorithm requires the needle tip deflection and its derivative. This signal is filtered by fitting polynomials to the deflection values. In these calculations, the lack of data points at the first moments of the experiment leads to a noisy response that may cause chattering. Consequently, the algorithm is ignored for the first few seconds as far as switching the needle orientation is considered. To find the switching parameters, a conservative estimate of needle curvature $k_0 = 10^{-3}$ 1/mm is used.

In the first two sets of experiments we want the needle to be controlled on a straight path, i.e. $y_d = 0$, with different values of switching thresholds. In addition, since the desired performance is to reach the target point on a straight line, the needle tip angle will be limited to small values, we choose θ^* to be 0.03 rad which leads to $s_s < 1.34$. In the first and second set of experiments, we have chosen $s_s = 1$ and $s_s = 0.5$, respectively. The results are displayed in Fig. 5. The number of rotations and the error values are summarized in Table II. The experiments show that for $s_s = 1$ and $s = 0.5$ in 15% mixture tissue, the mean absolute error is 0.62 ± 0.39 mm and 0.47 ± 0.31 mm, with the maximum targeting error of 1.23 mm and 0.91 mm, respectively. As we can see, reducing the switching threshold from 1 to 0.5, causes a decrease of 0.12 mm in the mean error and an increase of 3 in the maximum number of rotations between different trials. In third set of experiments, the insertion velocity is increased from $v = 2$ mm/sec to $v = 4$ mm/sec and accordingly the value of the parameter b is updated to 8. As stated in section III, smaller b leads to a faster error dynamic equation that makes the error tend zero faster. In this case the mean absolute error is 0.37 ± 0.34 mm with the maximum targeting error of 0.89 mm.

In order to study the effect of the tissue on the system's performance, in the next set of experiments the weight ratio of gelatin to water is increased from 15% to 20%. The results are shown in Fig. 5(g) and 5(h). Since the switching threshold is determined according to Equation (21), the deflection error will not change with the change in the tissue properties. However, the number of rotations depend on how fast the sliding surface, which is a function of the needle deflection, reaches the switching thresholds and is therefore affected by a change in tissue properties. A stiffer tissue can cause more deflection as the needle is inserted and consequently the number of rotations increases. Comparing the result in TableII, it can be seen that the error for 20% mixture is comparable with that for the 15% mixture but the average number of rotations is slightly more as the higher weight ratio leads to a stiffer tissue, which results in more needle deflection. The next set of experiments involve steering the needle tip to reach a target regardless of its path which is the case for applications such as biopsy. According to equation (21), the

value of $s(0) = ce(0)$) should be considered in determining s_s. Moreover, in such a condition, the needle should be allowed to deflect more to reach the desired deflection y_d, and θ^* should be selected larger, which leads to different values for b and c. By choosing a feasible value of θ^*, other parameters can be found. Here, for $y_d = -2$ mm and $\theta^* = 0.05$ rad, we have chosen $b = 25$ and $c = 1$, which satisfy (11) and leads to $s_s < 1.74$ from which s_s is selected to be 1. The results in Table II show the mean absolute error of 0.67 ± 0.75 mm with the maximum targeting error of 0.58 mm. In the last set of experiments, the biological tissue (pork) is embedded into gelatin used in the first set of experiments in order to simulate a 2-layer biological tissue. In these experiments, the tissue is nonhomogeneous as the first layer is gelatin and the second layer is biological tissue (pork), which itself has different layers. Fig. 5(k),5(l) and Table II show the results with mean absolute error of 0.51 ± 0.32 mm and the maximum targeting error of 1.76 mm. The results show the insensitivity of the proposed method to tissue parameters, meaning that the proposed algorithm has the capability of being used in real tissue with different and nonhomogeneous layers.

From Fig.5 it can be seen that there is a significant difference between the trials. This can be caused by the needle tip initial condition. The difference between the trials can be caused by the needle tip initial condition. Though it is attempted to have the initial angle equal to zero for all trials, it is difficult to account for and adjust. Moreover, the insertions may be affected by the tracks made in the tissue caused by previous insertions. Having said the above, the results show the insensitivity of the method to such uncertainties.

In all of the experiments the maximum value of error is less than 2 mm which is the size of the smallest lesion that can be detected by ultrasound images [12]. Moreover the maximum number of rotation obtained in these experiments is comparable to other methods proposed in literature [24].

V. Discussion

A. Comparison

The duty cycle spinning is a technique of simultaneously inserting and rotating the needle, enabling it move on paths with different curvatures. Many control methods proposed in the literature have combined this technique with different planning methods for needle steering. In this method, the needle is inserted and rotated for the time duration T_{rot} ant is inserted for the time duration T_{ins}. The duty cycle factor α is defined as the ratio between these two periods as

$$\alpha = \frac{T_{rot}}{T_{rot} + T_{ins}} \tag{22}$$

This factor determines the relation between the desired curvature k_{des} and the maximum needle curvature k_{max} as

$$k_{des} = k_{max}(1 - \alpha) \tag{23}$$

However, to find α, both k_{max} and k_{des} should be known. k_{max} can be found by pre-operative insertions and by fitting circles to the needle path and k_{des} should be determined by path planning methods. As stated before, for brachytherapy application, it is desired to keep the needle moving on a straight path. For a straight line path with minimum curvature ($k_{des} = 0$), α equals 1 which is equivalent to $T_{ins} = 0$ or continuously rotating the needle. This leads to a large number of rotations and potentially excessive tissue trauma. Moreover, this method requires an exact estimation of the maximum curvature k_{max}, which may be variable during the insertion due to tissue in-homogeneity. The method presented in this paper does not require any accurate estimation of curvature as some conservative value of it can be employed to determine the switching parameters. Besides, for regulating the needle position to a stationary point, no planning is needed. Moreover, the number of switches can be reduced by increasing the value of switching threshold s_s and accepting some reasonable values of error.

B. Practical issues

For safety reasons, it is always desired to involve the clinician in the loop. Examples of such involvement can be found in human in the loop needle insertions [25]. In robot-assisted procedures we envision, the steering action is divided between the robot and the clinician to hit the right balance between improving the targeting accuracy of insertions and the treatment safety issues. In the paper, we have also automated the needle insertion only for repeatability of the trails. There is absolutely no reason the proposed method cannot be used in robot-assisted procedures where the control action in the steering algorithm is the needle axial rotation while the other degree of freedom of the system, which is the insertion velocity, can be commanded directly by the clinician. In other words, the steering algorithm is only there to find and implement the best rotations as the insertion is performed by the clinician.

VI. Conclusion

In this paper we have proposed a control structure for steering flexible beveled-tip needles toward fixed points in soft tissue. Two possible bevel orientations (0° and 180°) are considered for the needle, which lead to a switching control system with two modes. As a feedback system, the controller is supplied with the needle deflection error obtained from ultrasound images and constructs the control law to switch the system to the proper mode for reducing the targeting error. Using kinematic unicycle equations for the needle, the constraints on switching parameters are derived to ensure the stability of the system and convergence of the error. The experiments are performed on phantom tissues and biological tissue using an experimental setup. From the experiments in phantom tissue, the maximum average error of 0.62 ± 0.39 mm with a maximum number of rotations of 6 and for the biological tissue the average error of 0.51 ± 0.32 mm with the maximum number of rotations of 7 are obtained.

In this work, the target location is considered to be stationary and no obstacles are considered. Although this method can be used in environments with obstacles by properly selecting the initial insertion point, further developments and

TABLE II
SUMMARY OF THE EXPERIMENTAL RESUTLS

	System Parameters						Results						
#	Tissue	b	c	V_{ins} [mm/sec]	s_s	y_d [mm]	Min # of rotation	Max # of rotations	Mean Absolute Error [mm]	σ	RMSE [mm]	Mean Max Error [mm]	Max Targeting Error [mm]
1	gelatin 15%	15	1	2	1	0	3	6	0.62	0.39	0.0014	1.39	1.23
2	gelatin 15%	15	1	2	0.5	0	5	9	0.47	0.31	0.008	1.14	0.91
3	gelatin 15%	8	1	4	1	0	4	5	0.37	0.34	0.002	1.01	0.89
4	gelatin 20%	15	1	2	1	0	5	7	0.46	0.33	0.0005	1.13	1.16
5	gelatin 15%	25	1	2	0.8	-2	4	7	0.67	0.75	0.05	2.1	0.58
6	biological	15	1	2	1	0	3	7	0.51	0.32	0.003	1.12	1.76

experiments are required to verify the performance of the proposed structure for having obstacles, moving targets, trajectory tracking in the presence of obstacles and control both in and out of plane deflections to steer the needle to any feasible point in the 3D environment.

REFERENCES

[1] R. Alterovitz, K. Goldberg, and A. Okamura, "Planning for steerable bevel-tip needle insertion through 2d soft tissue with obstacles," in *Proceedings of the 2005 IEEE International Conference on Robotics and Automation, 2005. ICRA 2005.* IEEE, 2005, pp. 1640–1645.

[2] R. Alterovitz, A. Lim, K. Goldberg, G. S. Chirikjian, and A. M. Okamura, "Steering flexible needles under markov motion uncertainty," in *IEEE/RSJ International Conference on Intelligent Robots and Systems, 2005.(IROS 2005). 2005.* IEEE, 2005, pp. 1570–1575.

[3] R. Alterovitz, M. Branicky, and K. Goldberg, "Constant-curvature motion planning under uncertainty with applications in image-guided medical needle steering," in *Algorithmic Foundation of Robotics VII*. Springer, 2008, pp. 319–334.

[4] W. Park, J. S. Kim, Y. Zhou, N. J. Cowan, A. M. Okamura, and G. S. Chirikjian, "Diffusion-based motion planning for a nonholonomic flexible needle model," in *Proceedings of the 2005 IEEE International Conference on Robotics and Automation, 2005. ICRA 2005.* IEEE, 2005, pp. 4600–4605.

[5] J. Xu, V. Duindam, R. Alterovitz, and K. Goldberg, "Motion planning for steerable needles in 3d environments with obstacles using rapidly-exploring random trees and backchaining," in *IEEE International Conference on Automation Science and Engineering, 2008. CASE 2008.* IEEE, 2008, pp. 41–46.

[6] V. Duindam, R. Alterovitz, S. Sastry, and K. Goldberg, "Screw-based motion planning for bevel-tip flexible needles in 3d environments with obstacles," in *IEEE International Conference on Robotics and Automation, 2008. ICRA 2008.* IEEE, 2008, pp. 2483–2488.

[7] K. B. Reed, V. Kallem, R. Alterovitz, K. Goldbergxz, A. M. Okamura, and N. J. Cowan, "Integrated planning and image-guided control for planar needle steering," in *2nd IEEE RAS & EMBS International Conference on Biomedical Robotics and Biomechatronics, 2008. BioRob 2008.* IEEE, 2008, pp. 819–824.

[8] D. S. Minhas, J. A. Engh, M. M. Fenske, and C. N. Riviere, "Modeling of needle steering via duty-cycled spinning," in *Engineering in Medicine and Biology Society, 2007. EMBS 2007. 29th Annual International Conference of the IEEE.* IEEE, 2007, pp. 2756–2759.

[9] A. Majewicz, J. J. Siegel, A. A. Stanley, and A. M. Okamura, "Design and evaluation of duty-cycling steering algorithms for robotically-driven steerable needles," in *IEEE International Conference on Robotics and Automation (ICRA), 2014*. IEEE, 2014, pp. 5883–5888.

[10] S. Patil and R. Alterovitz, "Interactive motion planning for steerable needles in 3d environments with obstacles," in *3rd IEEE RAS and EMBS International Conference on Biomedical Robotics and Biomechatronics (BioRob), 2010*. IEEE, 2010, pp. 893–899.

[11] M. Abayazid, M. Kemp, and S. Misra, "3d flexible needle steering in soft-tissue phantoms using fiber bragg grating sensors," in *IEEE International Conference on Robotics and Automation (ICRA), 2013*. IEEE, 2013, pp. 5843–5849.

[12] P. Moreira and S. Misra, "Biomechanics-based curvature estimation for ultrasound-guided flexible needle steering in biological tissues," *Annals of biomedical engineering*, pp. 1–11, 2014.

[13] D. C. Rucker, J. Das, H. B. Gilbert, P. J. Swaney, M. I. Miga, N. Sarkar, and R. J. Webster, "Sliding mode control of steerable needles," 2013.

[14] N. Shahriari, E. Hekman, M. Oudkerk, and S. Misra, "Design and evaluation of a computed tomography (ct)-compatible needle insertion device using an electromagnetic tracking system and ct images," *International journal of computer assisted radiology and surgery*, pp. 1–8, 2015.

[15] N. Abolhassani, R. V. Patel, and F. Ayazi, "Minimization of needle deflection in robot-assisted percutaneous therapy," *The international journal of medical Robotics and computer assisted surgery*, vol. 3, no. 2, pp. 140–148, 2007.

[16] P. Moreira, R. Patil, R. Alterovitz, and S. Misra, "Needle steering in biological tissue using ultrasound-base online curvature estimation," in *& International Conference on Robotics and Automation (ICRA), 2014.* IEEE, 2014.

[17] R. J. Webster, J. S. Kim, N. J. Cowan, G. S. Chirikjian, and A. M. Okamura, "Nonholonomic modeling of needle steering," *The International Journal of Robotics Research*, vol. 25, no. 5-6, pp. 509–525, 2006.

[18] V. Utkin *et al.*, "Sliding mode control design principles and applications to electric drives," *IEEE Transactions on Industrial Electronics*, vol. 40, no. 1, pp. 23–36, 1993.

[19] T. Podder, D. Clark, D. Fuller, J. Sherman, W. Ng, L. Liao, D. Rubens, J. Strang, E. Messing, Y. Zhang *et al.*, "Effects of velocity modulation during surgical needle insertion," in *IEEE-EMBS 2005. 27th Annual International Conference of the Engineering in Medicine and Biology Society, 2005.* IEEE, 2005, pp. 5766–5770.

[20] P. J. Swaney, J. Burgner, H. B. Gilbert, and R. J. Webster, "A flexure-based steerable needle: high curvature with reduced tissue damage," *IEEE Transactions on Biomedical Engineering*, vol. 60, no. 4, pp. 906–909, 2013.

[21] T. Lehmann, M. Tavakoli, N. Usmani, and R. Sloboda, "Force-sensor-based estimation of needle tip deflection in brachytherapy," *Journal of Sensors*, vol. 2013, 2013.

[22] M. Waine, C. Rossa, R. Sloboda, N. Usmani, and M. Tavakoli, "3d shape visualization of curved needles in tissue from 2d ultrasound images using ransac," in *IEEE International Conference on Robotics and Automation (ICRA), 2015*. IEEE, 2015, pp. 4723–4728.

[23] M. Abayazid, P. Moreira, N. Shahriari, S. Patil, R. Alterovitz, and S. Misra, "Ultrasound-guided three-dimensional needle steering in biological tissue with curved surfaces," *Medical engineering & physics*, vol. 37, no. 1, pp. 145–150, 2015.

[24] M. Abayazid, G. J. Vrooijink, S. Patil, R. Alterovitz, and S. Misra, "Experimental evaluation of ultrasound-guided 3d needle steering in biological tissue," *International journal of computer assisted radiology and surgery*, vol. 9, no. 6, pp. 931–939, 2014.

[25] C. Pacchierotti, M. Abayazid, S. Misra, and D. Prattichizzo, "Teleoperation of steerable flexible needles by combining kinesthetic and vibratory feedback," *IEEE Transactions on Haptics*, vol. 7, no. 4, pp. 551–556, 2014.

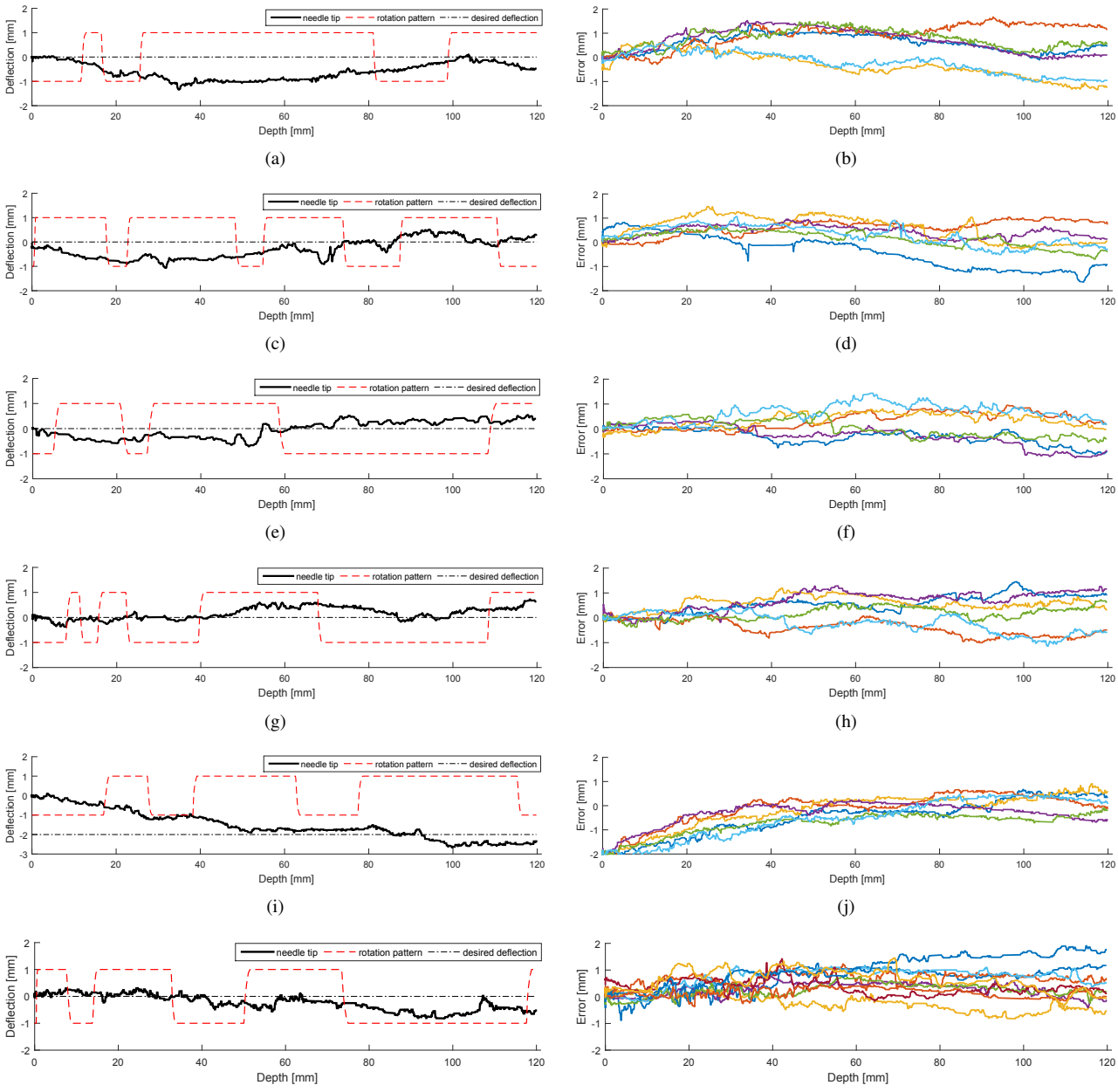

Fig. 5. Experimental results for needle insertion. (a),(b) for gelatin tissue with $b = 15$, $c = 1$, $s_s = 1$, $y_d = 0\,mm$, $v_{ins} = 2\,mm/sec$ and 15% tissue mixture. (c),(d) for gelatin tissue with $b = 15$, $c = 1$, $s_s = 0.5$, $y_d = 0\,mm$, $v_{ins} = 2\,mm/sec$ and 15% tissue mixture. (e),(f) for gelatin tissue with $b = 8$, $c = 1$, $s_s = 1$, $y_d = 0\,mm$, $v_{ins} = 4\,mm/sec$ and 15% tissue mixture. (g),(h) for gelatin tissue with $b = 15$, $c = 1$, $s_s = 1$, $y_d = 0\,mm$, $v_{ins} = 2\,mm/sec$ and 20% tissue mixture. (i),(j) for gelatin tissue with $b = 25$, $c = 1$, $s_s = 0.8$, $y_d = -2\,mm$, $v_{ins} = 2\,mm/sec$ and 15% tissue mixture. (k),(l) for biological tissue embedded in 15% gelatin mixture with $b = 15$, $c = 1$, $s_s = 1$, $y_d = 0\,mm$ and $v_{ins} = 2\,mm/sec$. (a), (c), (e), (g), (i), (k) demonstrate one of the insertion trials as well as the rotation pattern obtained from controller. (b), (d), (f), (h), (j), (l) show the deflection error for the tials.